Appl Phys B (2010) 99: 553–558
DOI 10.1007/s00340-010-3930-0

Applied Physics B
Lasers and Optics

Modeling and analysis of birefringence in magneto-optical thin film made by SiO_2/ZrO_2 doped with ferrite of cobalt

A. Hocini · T. Boumaza · M. Bouchemat · F. Choueikani · F. Royer · J.J. Rousseau

Received: 3 September 2009 / Revised version: 13 December 2009 / Published online: 2 March 2010

Abstract The zero-birefringence condition is an important requirement for magneto-optical waveguide devices. It has been analyzed by means of Film Mode Matching method (FMM). The modelling is based on geometrical adjustments of the rib waveguide and especially the etch depth, which is a critical parameter in the design of rib waveguide. We determine the waveguide dimensions that would allow the same propagation constants for both polarizations TE and TM, and we have found that there are more choices for waveguide dimensions to produce birefringence-free waveguides and single-mode rib waveguide simultaneously.

1 Introduction

More and more, the sol–gel process gives a solution to fabricate integrated optic devices. It is considered as a versatile, flexible and a low-cost technique useful for the realization of integrated photonic devices [1–5].

Many functions are needed in optical processing to be integrated. Among these functions are optical waveguide isolators and modulators that have a nonreciprocal effect and are very important in optical network systems. Isolators are used in the high-speed fiber transmission systems to stabilize the laser diodes by protecting them from unwanted light reflections running back on the line [2].

Currently, only bulk forms of these components made of garnet oxide crystals are commercially available, and integrated versions are highly desirable. The use of magnetic nanoparticles as a magneto-optical active element in a silica-based matrix prepared via sol–gel process has been discussed in a large number of papers, from first of these [3] to the most recent [4]. This latter is prepared via organic–inorganic process. The attractivity of such approach lies in the full compatibility of the sol–gel coating with classical integrated technologies and especially the technology on glass. Indeed, crystallized magnetic nanoparticles are dispersed in the sol–gel liquid preparation before the coating, and, thus, contrarily to classical techniques, high temperature is not required to obtain a magnetic behavior. Furthermore, this elaboration method is easy to implement and provide magneto-optical thin films with a refractive index value (1.5) close to that of other integrated optical devices. The inherent low refractive index contrast between the film and the substrate in sol–gel organic–inorganic waveguides, combined with a thickness larger than that of classical magneto-optical waveguides, should allow an efficient fiber coupling, which is highly desirable for laser-waveguide coupling [2, 4].

Magneto-optical waveguides are the basic elements for nonreciprocal integrated optics; the phase matching between the fundamental TE and TM modes is an essential condition in magneto-optical waveguides. We have adopted the method of controlling the dimensions (width and etching depth). The problem of thin-film phase mismatch between TE and TM modes ($\Delta\beta = \beta_{TE} - \beta_{TM} = 2\pi\,\Delta Nm/\lambda$, where ΔNm is the modal birefringence) affects with Faraday ro-

A. Hocini (✉)
Département d'Électronique, Université de M'sila, 28000 M'sila, Algeria
e-mail: hocini74@yahoo.fr
Fax: +213-35-552441

A. Hocini · T. Boumaza · M. Bouchemat
Laboratoire Micro Systèmes et Instrumentation, Département d'Électronique, Université de Constantine, route d'Aïn el Bey, Constantine, Algeria

F. Choueikani · F. Royer · J.J. Rousseau
Laboratoire Dispositifs et Instrumentation en Optoélectronique et Micro-ondes—EA 3523, Université Jean Monnet, 21 rue Paul Michelon, 42023 St Etienne Cedex 2, France

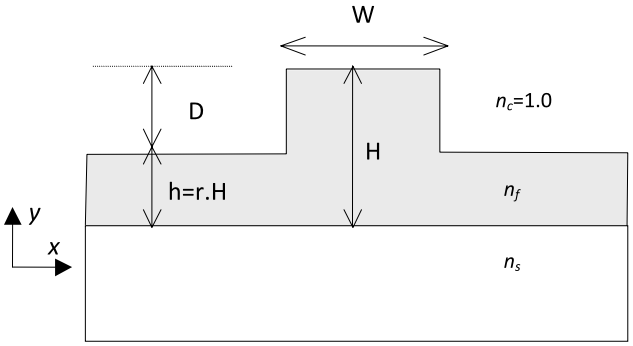

Fig. 1 Schematic representation of a Rib waveguide. Structural parameters are the height H and the width W and refractive-index n_s, n_f, and n_c. x and y denote the cross section coordinate axes, with the y-direction parallel to the substrate surface. The light beam propagation is along Oz

tation the conversion efficiency in these films, which is expressed as [5]

$$R = \frac{\theta_F^2}{\theta_F^2 + (\Delta\beta/2)^2}, \tag{1}$$

$\theta_F(^\circ/\text{cm})$ is the specific Faraday rotation of the material constituting the waveguide.

The present work describes the design rule that must be imposed to the geometry of such device to make them behave as single-mode and phase-matched rib waveguides. It consists of the tuning of the geometrical parameters (height, width, and etching depth); see Fig. 1.

2 Design

Magneto-optical waveguides are the key elements of nonreciprocal devices which perform guiding, isolating, modulating, and circulating of optical signal. Design and simulation become very important before fabrication; the film mode matching (FMM) method by Sudbo [6] has been used to study the influence of the geometrical parameters for the waveguide. The device is shown schematically in Fig. 1, where W is the rib width, H is the inner rib height, and r is the fractional height of the side regions compared to the rib center (the outer–inner ratio). For a better understanding, we will also consider the etching depth $D = H(1 - r)$, which directly gives the edge height of the rib waveguide. We have chosen waveguide optical parameters corresponding to SiO_2/ZrO_2 film doped with ferrite of cobalt. The indices of the film ($n_f = 1.513$ at $\lambda = 820$ nm and $n_f = 1.509$ at $\lambda = 1550$ nm) on Pyrex substrate ($n_s = 1.472$ at $\lambda = 632.8$ nm) are adjusted for each wavelength [4, 7].

The magneto-optical thin film is inherently suffering from birefringence (ΔNm around 1×10^{-4} at $\lambda = 820$ nm and 2.7×10^{-4} at $\lambda = 1550$ nm) for planar waveguide [4]. However, the formation of two-dimensional structures to provide 2-D optical confinement induces modal birefringence due to the difference in effective indices for horizontally polarized modes (HE, i.e., quasi-TE) and vertically polarized modes (EH, i.e., quasi-TM) [8].

In order to design a waveguide with zero-birefringence, the first step was to investigate the polarization characteristics of the rib waveguide due to its geometry.

The software, based on the film mode matching (FMM) method, has been used to study the influence of the geometrical parameters for the waveguide described above.

All the modes propagating in the rib waveguide are calculated for both TE and TM polarizations, and the corresponding effective index (neff) and propagation constant β are determined.

The waveguide birefringence is defined as the difference between the effective indexes of two orthogonally polarized modes, the horizontally polarized mode (quasi-TE) and the vertically polarized mode (quasi-TM) $\Delta N = N_{\text{TE}} - N_{\text{TM}}$. In order to obtain zero-birefringence in rib waveguide, an optimization of waveguide dimensions is necessary.

3 Geometrical influence

The FIMMWAVE [9] simulation package was used to simulate the waveguide structure. The initial height is set to $H = 3$ μm; this dimension was chosen in order to maintain as large a device as possible for ease of coupling light to the device. Using FIMMWAVE, the effective indices of the fundamental TE and TM waveguide modes were monitored as the width W and the parameter r (Fig. 1) were varied at wavelength $\lambda = 0.633$, 0.820, and 1.55 μm.

The iteration of the simulation was repeated for a given values of the parameter r(etch depth). Hence, the process is one in which we determine the effective indices of the fundamental TE and TM waveguide modes as the waveguide width is gradually increased, and a series of ΔN points were calculated.

Figures 2, 3 and 4 show a plot of the birefringence as a function of the normalized ratio width/wavelength (W/λ) for different values of the parameter r. The results show that for smaller values of etch depths ($r > 0.4$), the birefringence is always positive, and consequently the fundamental quasi-TE and quasi-TM waveguide modes cannot be equalized by varying values of waveguide width. As the parameter r decreases (etch depth increases), a tendency for two specific values of waveguide widths for which the effective index of the fundamental quasi-TE and quasi-TM waveguide modes can be equalized. This means that the zero-birefringence condition can be realized for two different waveguide widths when a deeper etch is employed [10]. The intersection of the

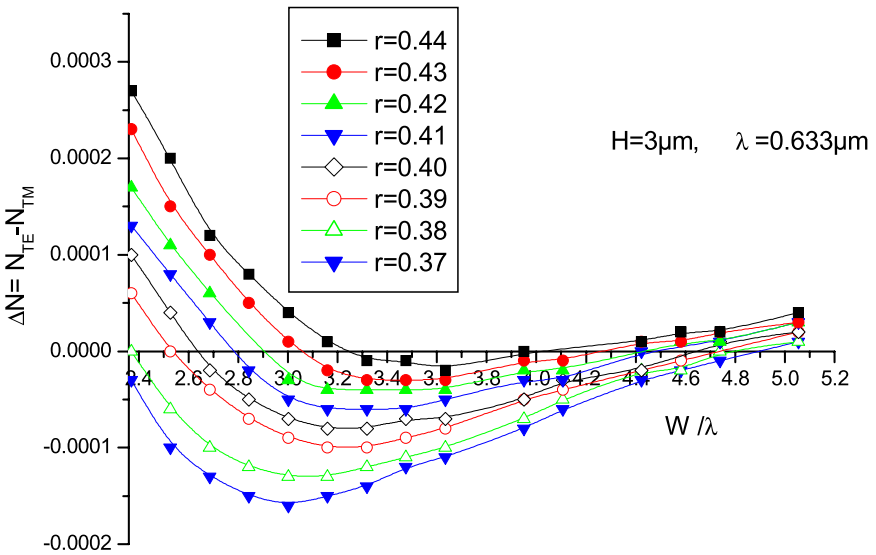

Fig. 2 Effective-index difference calculation between quasi-TE and quasi-TM polarized modes using FMM [9], for waveguide height $H = 3.00$ μm at $\lambda = 633$ nm

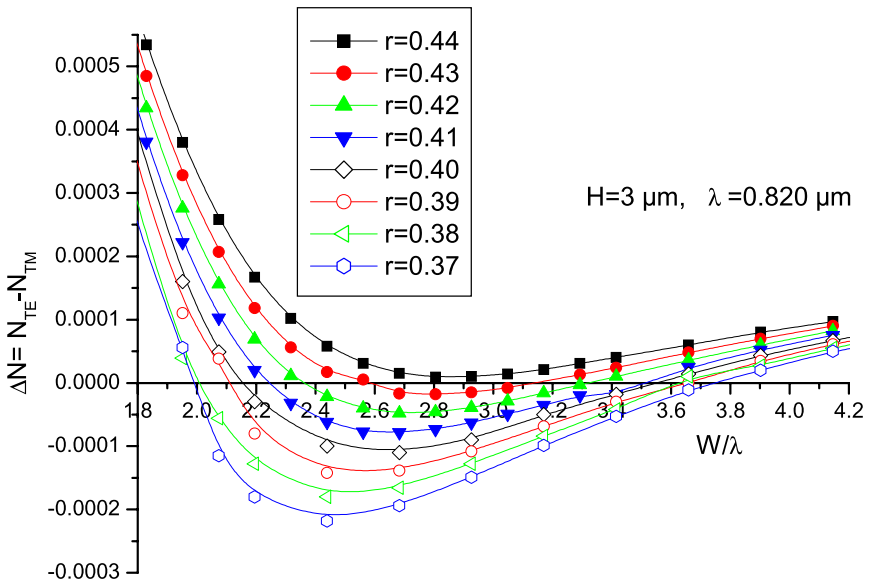

Fig. 3 Effective-index difference calculation between quasi-TE and quasi-TM polarized modes using FMM [9], for waveguide height $H = 3.00$ μm at $\lambda = 820$ nm

curves with the axe zero indicates that both TE and TM polarizations have the same effective index, and therefore the waveguide is phase matched in terms of propagation constant.

The degree of the influence of the waveguide width and the etch depth on phase matching condition for several wavelength is studied for $\lambda = 633$, 820, and 1550 nm. For each wavelength value, we have evaluated the propagation constant, and the etch depth D for both fundamental TE and TM polarizations are determined for different waveguide widths W in order to obtain phase-matched rib waveguide.

The intersections of the three curves with axe of zero-birefringence are used to study the variation of the parameter r as a function of the width W in order to obtain phase matching condition. Figure 5 shows clearly that the parameter r, corresponding to the phase matching condition, increases (or etch depth D decreases) according to the decrease of the wavelength. The maximum of r (corresponding to minimum of etching depth) is observed for each curve.

Next, it was necessary to design a single-mode rib waveguide, which is an important requirement for optical waveguide devices, because almost every kind of active and passive integrated optic device is designed to substate only the fundamental mode of propagation for use with optical fibers.

First, we fixed the rib-waveguide height parameter H, etch depth D (parameter r), and slab height h of the waveguide and changed the waveguide width to find the single-mode–multimode boundary. The iteration of the simulation is repeated with different values of the slab height

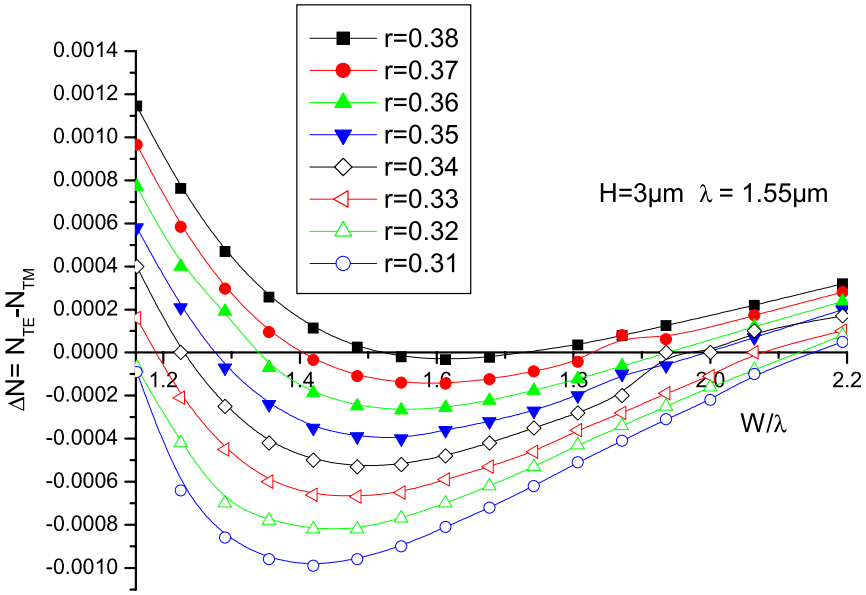

Fig. 4 Effective-index difference calculation between quasi-TE and quasi-TM polarized modes using FMM [9], for waveguide height $H = 3.00$ μm at $\lambda = 1550$ nm

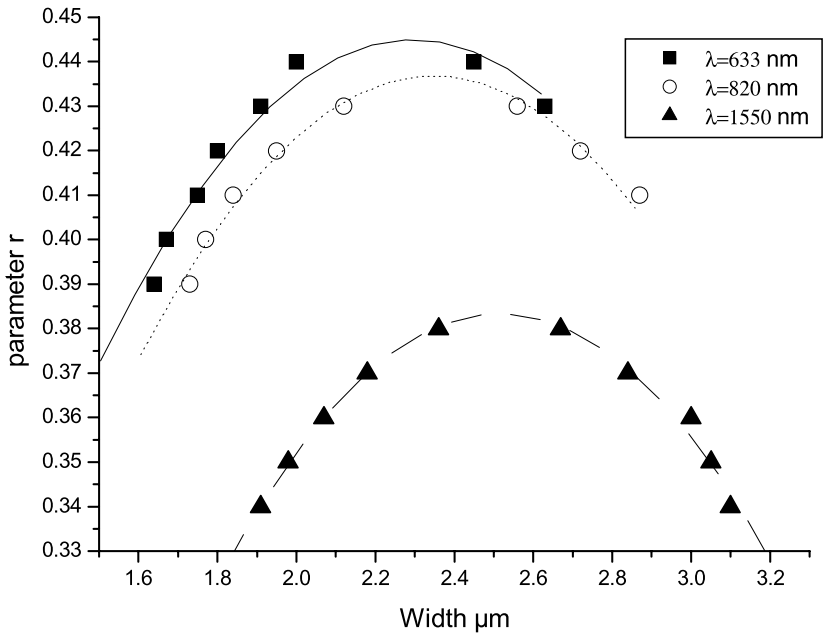

Fig. 5 Waveguide width influence on parameter r in the structure to support zero birefringence for waveguide height $H = 3.00$ μm, at $\lambda = 633$, 820, and 1550 nm

h to waveguide height ratio parameter r $(r = h/H)$, the process is to gradually increase the waveguide width until a second-mode propagation, and we determine the maximum waveguide width to reach single-mode operation for both polarization TE and TM. This was done for a given value of wavelength. Figure 5 shows also a typical result of modeling the estimate of a single-mode with a width equal to W (the cut-off condition for the second mode).

The maximum width to keep a single-mode waveguide increases as the wavelength increases, the last right point of the three curves determines the maximum value of the width to remain at the single-mode region. It was found that for $\lambda = 633$ nm, the maximum width for monomode waveguide is $W_{\max} = 2.60$ μm, for $\lambda = 820$ nm the $W_{\max} = 2.90$ μm, and for $\lambda = 1550$ nm, $W_{\max} = 3.20$ μm.

It is clear that it is possible to produce birefringence-free waveguides and single-mode rib waveguides simultaneously for some of the geometries and dimensions when a deeper etch depth is employed. There are more choices for waveguide dimensions that fulfil the two conditions simultaneously at $\lambda = 1550$ nm.

Similar to the calculation of zero-birefringence and single-mode conditions at $H = 3$ μm, other values of height are also used in the simulation to show the influence of this

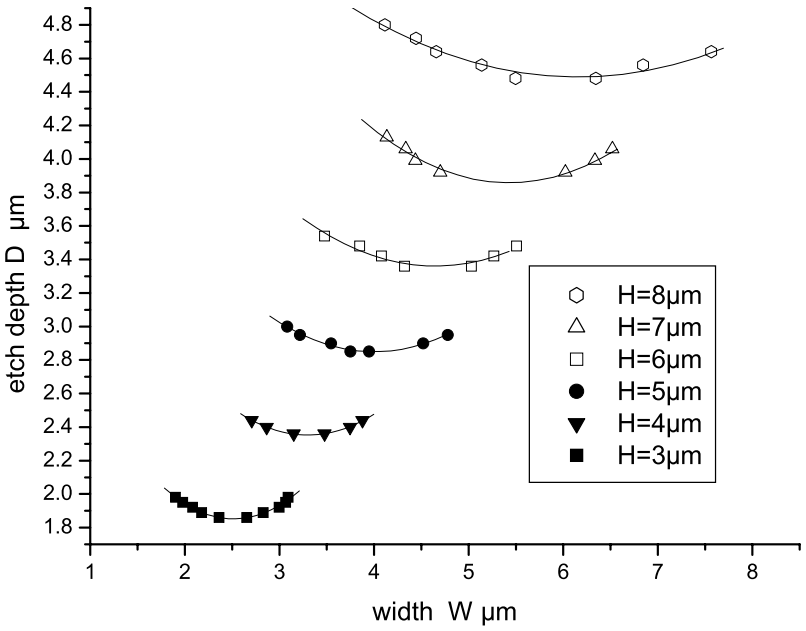

Fig. 6 Waveguide width influence on etching depth in the structure to support zero birefringence for waveguide heights $H = 3.00$, 4.00, 5.00, 6.00, 7.00, and 8.00 µm at $\lambda = 1550$ nm

parameter on the modal birefringence and the single-mode condition.

From Fig. 4, all the points which cross the zero-birefringence axis for rib waveguide height parameter of $H = 3.00$ µm and $\lambda = 1550$ nm are used to study the influence of the waveguide width on the etch depth D corresponding to $\Delta N = 0$, the variation of the etch depth is shown in Fig. 6 at $\lambda = 1550$ nm. The calculated points are fitted by a polynomial of degree 2; we also added simulated zero-birefringence data for waveguide height of 4.00, 5.00, 6.00, 7.00, and 8.00 µm, and we observed similar trends for all rib waveguide heights.

There are three important things that can be seen in Fig. 6. First, as the height H increases, the etch depth (D) decreases (parameter r increases); this can be observed for all the phase matching data points. Second, there are more choices for the waveguide dimensions that fulfil the two conditions simultaneously. Third, the most important is that there is a minimum of each depth $D_{\min}$ for each waveguide, and if we assume that the relationship between the etch depth and waveguide height is approximately linear, the following equations describe the minimum etch depth for a given waveguide rib height to predict phase matching condition after linear fitting of simulation data:

$$D_{\min} = 0.062 + 0.54H \text{ [µm]} \quad \text{for } \lambda = 820 \text{ nm}, \tag{2}$$

$$D_{\min} = 0.24 + 0.54H \text{ [µm]} \quad \text{for } \lambda = 1550 \text{ nm}. \tag{3}$$

For all six curves, we note that the last right point determines the limits width to have single-mode waveguide for $\lambda = 1550$ nm whose rib width W and etching depth D given in Table 1 correspond to zero-birefringence condition.

Table 1 Rib waveguide dimensions corresponding to Zero-birefringence and single-mode conditions at $\lambda = 1550$ nm; width W and etching depth D are given for height H ranging from 3.00 µm to 8.00 µm

H (µm)	3.00	4.00	5.00	6.00	7.00	8.00
W (µm)	3.09	3.87	4.78	5.50	6.52	7.56
D (µm)	1.98	2.44	2.95	3.48	4.06	4.64

4 Conclusion

An analysis of the modal birefringence between the TE and TM guided modes in SiO_2/ZrO_2 thin film doped with ferrite of cobalt has been presented using mode solver program to provide theoretical prediction that certain waveguide geometries can lead to zero-birefringence and single-mode performance; the etching depth, width, and height values have been determined to design waveguides which fulfil this condition, for wavelength 0.633, 0.820, and 1.55 µm.

In the rib waveguide, it has been shown that the zero-birefringence condition is valid only for deeply etched waveguides, and we have found that there are more choices for waveguide dimensions that fulfil the two conditions simultaneously at $\lambda = 1550$ nm.

In the future, such structure can find a wide application in optoelectronic devices, and it may be interesting to realize waveguides made of magnetophotonic crystals.

References

1. A. Chiappini, C. Armellini, A. Chiasera, M. Ferrari, R. Guider, Y. Jestin, L. Minati, E. Moser, G. Nunzi Conti, S. Pelli, R. Retoux,

G.C. Righini, G. Speranza, Journal of Non-Crystalline Solids **355**, 1132 (2009)
2. F. Royer, D. Jamon, J.J. Rousseau, H. Roux, D. Zins, V. Cabuil, Appl. Phys. Lett. **86**, 011107 (2005)
3. M.F. Bentivegna, M. Nyvlt, J. Ferre, J.P. Jamet, A. Brun, S. Visnovsky, R. Urban, J. Appl. Phys. **58**, 2270 (1999)
4. F. Choueikani, F. Royer, D. Jamon, A. Siblini, J.J. Rousseau, S. Neveu, J. Charara, Appl. Phys. Lett. **94**, 051113 (2009)
5. V. Zayets, M.C. Debnath, K. Ando, Appl. Phys. Lett. **84**, 565 (2004)
6. A.Sv. Sudbø, IEEE Photonics Technol. Lett. **5**, 342 (1993)
7. F. Chouikani, Étude des potentialités de couches minces sol–gel dopées par des nanoparticules magnétiques pour la réalisation de composants magnéto-optiques intégrés. Thèse de doctorat, Université de Saint-Étienne, 2008
8. S.P. Chan, V.M.N. Passaro, G.T. Reed, Electron. Lett. **41**, 9 (2005)
9. FIMMWAVE program, Photon Design Product. http://www.photond.com
10. A. Hocini, T. Boumaza, M. Bouchemat, F. Royer, D. Jamon, J.J. Rousseau, Microelectron. J. **39**, 99 (2008)